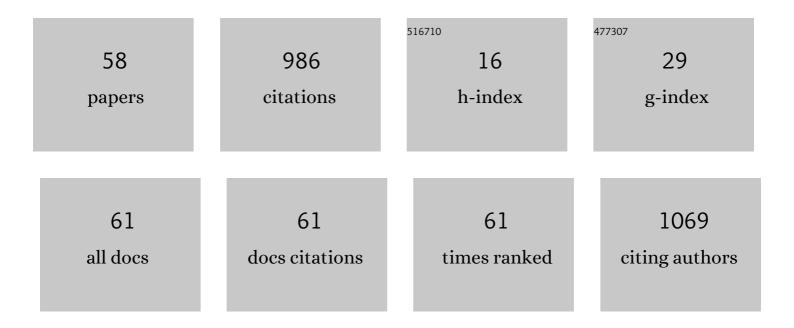
## Konstantin I Momot

List of Publications by Year in descending order

Source: https://exaly.com/author-pdf/5121910/publications.pdf Version: 2024-02-01



#	Article	IF	CITATIONS
1	Sensing mammographic density using single-sided portable Nuclear Magnetic Resonance. Saudi Journal of Biological Sciences, 2022, 29, 2447-2454.	3.8	3
2	Portable NMR for quantification of breast density in vivo: Proof-of-concept measurements and comparison with quantitative MRI. Magnetic Resonance Imaging, 2022, 92, 212-223.	1.8	2
3	Reorientational dynamics of molecules in liquid methane: A molecular dynamics simulation study. Journal of Molecular Liquids, 2021, 324, 114727.	4.9	4
4	RASSF1A Suppression as a Potential Regulator of Mechano-Pathobiology Associated with Mammographic Density in BRCA Mutation Carriers. Cancers, 2021, 13, 3251.	3.7	1
5	Mechanical Pressure Driving Proteoglycan Expression in Mammographic Density: a Self-perpetuating Cycle?. Journal of Mammary Gland Biology and Neoplasia, 2021, 26, 277-296.	2.7	2
6	Heparanase Promotes Syndecan-1 Expression to Mediate Fibrillar Collagen and Mammographic Density in Human Breast Tissue Cultured ex vivo. Frontiers in Cell and Developmental Biology, 2020, 8, 599.	3.7	14
7	Effects of Hydrogen Bonding on the Rotational Dynamics of Water-Like Molecules in Liquids: Insights from Molecular Dynamics Simulations. Australian Journal of Chemistry, 2020, 73, 734.	0.9	3
8	Quantification of breast tissue density: Correlation between single-sided portable NMR and micro-CT measurements. Magnetic Resonance Imaging, 2019, 62, 111-120.	1.8	12
9	Structure and Dynamics of Collagen Hydration Water from Molecular Dynamics Simulations: Implications of Temperature and Pressure. Journal of Physical Chemistry B, 2019, 123, 4901-4914.	2.6	17
10	Transverse relaxationâ€based assessment of mammographic density and breast tissue composition by singleâ€sided portable NMR. Magnetic Resonance in Medicine, 2019, 82, 1199-1213.	3.0	21
11	Assessment of collagen fiber orientation dispersion in articular cartilage by small-angle X-ray scattering and diffusion tensor imaging: Preliminary results. Magnetic Resonance Imaging, 2018, 48, 115-121.	1.8	6
12	Progression of Post-Traumatic Osteoarthritis in rat meniscectomy models: Comprehensive monitoring using MRI. Scientific Reports, 2018, 8, 6861.	3.3	15
13	T <sub>1</sub> â€based sensing of mammographic density using singleâ€sided portable <scp>NMR</scp> . Magnetic Resonance in Medicine, 2018, 80, 1243-1251.	3.0	25
14	Looking beyond the mammogram to assess mammographic density: A narrative review. Biomedical Spectroscopy and Imaging, 2018, 7, 63-80.	1.2	4
15	Anisotropic diffusion in stretched hydrogels containing erythrocytes: evidence of cellâ€shape distortion recorded by PGSE NMR spectroscopy. Magnetic Resonance in Chemistry, 2017, 55, 438-446.	1.9	10
16	Na + and solute diffusion in aqueous channels of Myverol bicontinuous cubic phase: PGSE NMR and computer modelling. Magnetic Resonance in Chemistry, 2017, 55, 464-471.	1.9	10
17	The distribution of the apparent diffusion coefficient as an indicator of the response to chemotherapeutics in ovarian tumour xenografts. Scientific Reports, 2017, 7, 42905.	3.3	16
18	Load-induced changes in the diffusion tensor of ovine anulus fibrosus: A pilot MRI study. Journal of Magnetic Resonance Imaging, 2017, 45, spcone-spcone.	3.4	0

Konstantin I Momot

#	Article	IF	CITATIONS
19	Loadâ€induced changes in the diffusion tensor of ovine anulus fibrosus: A pilot MRI study. Journal of Magnetic Resonance Imaging, 2017, 45, 1723-1735.	3.4	10
20	MRI magic-angle effect in femorotibial cartilages of the red kangaroo. Magnetic Resonance Imaging, 2017, 43, 66-73.	1.8	5
21	Rotational-Diffusion Propagator of the Intramolecular Proton–Proton Vector in Liquid Water: A Molecular Dynamics Study. Journal of Physical Chemistry B, 2017, 121, 10893-10905.	2.6	11
22	Magnetic resonance microimaging of cancer cell spheroid constructs. Biomedical Spectroscopy and Imaging, 2017, 5, 41-54.	1.2	6
23	Molecular Dynamics of a Hydrated Collagen Peptide: Insights into Rotational Motion and Residence Times of Single-Water Bridges in Collagen. Journal of Physical Chemistry B, 2016, 120, 12432-12443.	2.6	20
24	Introduction to Cartilage. New Developments in NMR, 2016, , 1-43.	0.1	5
25	Further development of discrete computational techniques for calculation of restricted diffusion propagators in porous media. Microporous and Mesoporous Materials, 2015, 205, 24-30.	4.4	1
26	Effect of Partial H2O-D2O Replacement on the Anisotropy of Transverse Proton Spin Relaxation in Bovine Articular Cartilage. PLoS ONE, 2014, 9, e115288.	2.5	31
27	Characterization of the Microarchitecture of Direct Writing Melt Electrospun Tissue Engineering Scaffolds Using Diffusion Tensor and Computed Tomography Microimaging. 3D Printing and Additive Manufacturing, 2014, 1, 95-103.	2.9	7
28	Simultaneous Magnetic Resonance Imaging and Consolidation Measurement of Articular Cartilage. Sensors, 2014, 14, 7940-7958.	3.8	21
29	A study of the diffusion characteristics of normal, delipidized and relipidized articular cartilage using magnetic resonance imaging. Journal of Materials Science: Materials in Medicine, 2013, 24, 1005-1013.	3.6	1
30	Diffusion tensor of water in partially aligned fibre networks. Journal Physics D: Applied Physics, 2013, 46, 455401.	2.8	20
31	Biomechanics of Synthetic Elastin: Insights from Magnetic Resonance Microimaging. Advanced Materials Research, 2013, 699, 457-463.	0.3	3
32	Diffusion-sensitive magnetic resonance spectroscopy and imaging in biomedical sciences. Biomedical Spectroscopy and Imaging, 2013, 2, 265-287.	1.2	3
33	Anatomical MR imaging of long bones: Comparative performance of MRI at 1.5 T and 3 T. Biomedical Spectroscopy and Imaging, 2013, 2, 21-35.	1.2	3
34	Langevin dynamics modeling of the water diffusion tensor in partially aligned collagen networks. Physical Review E, 2012, 86, 031917.	2.1	13
35	Microstructural magnetic resonance imaging of articular cartilage. Biomedical Spectroscopy and Imaging, 2012, 1, 27-37.	1.2	7
36	Sensitivity of the NMR density matrix to pulse sequence parameters: A simplified analytic approach. Journal of Magnetic Resonance, 2012, 221, 57-68.	2.1	1

Konstantin I Momot

#	Article	IF	CITATIONS
37	Quantification of the accuracy of MRI generated 3D models of long bones compared to CT generated 3D models. Medical Engineering and Physics, 2012, 34, 357-363.	1.7	101
38	Digital Processing of Diffusion-Tensor Images of Avascular Tissues. Biological and Medical Physics Series, 2011, , 341-371.	0.4	5
39	Diffusion tensor of water in model articular cartilage. European Biophysics Journal, 2011, 40, 81-91.	2.2	22
40	Anisotropy of spin relaxation of water protons in cartilage and tendon. NMR in Biomedicine, 2010, 23, 313-324.	2.8	42
41	Magnetic-Resonance Evaluation of the Suitability of Microstructured Polymer Optical Fibers As Sensors for Ionic Aqueous Solutions. ACS Applied Materials & Interfaces, 2009, 1, 197-203.	8.0	3
42	Anisotropy of collagen fibre alignment in bovine cartilage: comparison of polarised light microscopy and spatially resolved diffusion-tensor measurements. Osteoarthritis and Cartilage, 2008, 16, 689-697.	1.3	103
43	Inhomogeneous NMR Line Shape as a Probe of Microscopic Organization of Bicontinuous Cubic Phases. Journal of Physical Chemistry B, 2008, 112, 6636-6645.	2.6	7
44	PFG NMR diffusion experiments for complex systems. Concepts in Magnetic Resonance Part A: Bridging Education and Research, 2006, 28A, 249-269.	0.5	59
45	Convection-compensating diffusion experiments with phase-sensitive double-quantum filtering. Journal of Magnetic Resonance, 2005, 174, 229-236.	2.1	26
46	Acquisition of pure-phase diffusion spectra using oscillating-gradient spin echo. Journal of Magnetic Resonance, 2005, 176, 151-159.	2.1	11
47	Convection-compensating PGSE experiment incorporating excitation-sculpting water suppression (CONVEX). Journal of Magnetic Resonance, 2004, 169, 92-101.	2.1	37
48	Enhancement of Na+Diffusion in a Bicontinuous Cubic Phase by the Ionophore Monensin. Langmuir, 2004, 20, 2660-2666.	3.5	15
49	Pulsed field gradient nuclear magnetic resonance as a tool for studying drug delivery systems. Concepts in Magnetic Resonance, 2003, 19A, 51-64.	1.3	71
50	NMR Study of the Association of Propofol with Nonionic Surfactants. Langmuir, 2003, 19, 2088-2095.	3.5	76
51	Nuclear magnetic resonance radiation damping in inhomogeneous radio frequency fields: The toroid cavity detector. Journal of Chemical Physics, 2001, 115, 3992-4002.	3.0	3
52	Toroid Cavity Detectors for High-Resolution NMR Spectroscopy and Rotating Frame Imaging: Capabilities and Limitations. Journal of Magnetic Resonance, 2000, 142, 348-357.	2.1	14
53	Rate Constants and Thermodynamic Parameters of Rotation of Axial Ligands in a Bisligated Ferric Tetramesitylporphyrinate Complex Measured from the Temperature Dependence of1H Transverse Relaxation Rates. Journal of Physical Chemistry A, 1998, 102, 10682-10688.	2.5	8
54	Investigations of Rotation of Axial Ligands in Six-Coordinate Low-Spin Iron(III) Tetraphenylporphyrinates:  Measurement of Rate Constants from Saturation Transfer Experiments and Comparison to Molecular Mechanics Calculations. Journal of Physical Chemistry A, 1997, 101, 2787-2795.	2.5	29

#	Article	IF	CITATIONS
55	Proton NMR Relaxation in Six-Coordinate Low-Spin Iron(III) Tetraphenylporphyrinates:Â Temperature Dependence of Proton Relaxation Rates and Interpretation of NOESY Experiments. Journal of Physical Chemistry A, 1997, 101, 9207-9216.	2.5	14
56	Fourier Transform Ion Cyclotron Resonance Studies of Gas-Phase Reactions between Tungsten Ions and Hydrocarbons. Organometallics, 1994, 13, 2536-2538.	2.3	6
57	CHAPTER 3. Introduction to NMR and MRI. New Developments in NMR, 0, , 62-108.	0.1	1
58	CHAPTER 7. Quantification of Articular Cartilage Microstructure by the Analysis of the Diffusion Tensor. New Developments in NMR, 0, , 191-224.	0.1	0